

Two-proton alignment and shape changes in ^{65}Zn

B. Mukherjee, S. Muralithar, R. P. Singh, R. Kumar, K. Rani, and R. K. Bhowmik
Nuclear Science Centre, Aruna Asaf Ali Marg, Post Box 10502, New Delhi 67, India

S. C. Pancholi

Department of Physics and Astrophysics, Delhi University, Delhi 07, India

(Received 18 September 2000; revised manuscript received 19 March 2001; published 29 June 2001)

The nucleus $^{65}_{30}\text{Zn}$ was studied using the $^{52}\text{Cr}(^{16}\text{O}, 2pn)^{65}\text{Zn}$ reaction at a beam energy of 65 MeV. A rotational band built on the $g_{9/2}$ neutron orbital was observed to exhibit a band crossing at a rotational frequency of 0.6 MeV with an associated alignment of $7\hbar$. This alignment is interpreted as being due to a pair of $g_{9/2}$ protons. Total Routhian Surface calculations have been carried out which confirm that the shape of the nucleus changes from an oblate shape at low spin to a triaxial prolate shape at intermediate spin.

DOI: 10.1103/PhysRevC.64.024304

PACS number(s): 21.10.Re, 23.20.Lv, 25.70.Gh, 27.50.+e

I. INTRODUCTION

The study of high-spin states in atomic nuclei is a very active field, but little attention has been paid to light nuclei, say, $A \leq 65$. There are some experimental difficulties compared with the study of heavier nuclei; for example, γ -ray energies tend to be higher and recoil velocities are generally faster, which factors lead to a reduced detection efficiency and Doppler broadening problems. Further, because of the low Coulomb barrier in light nuclei, competition between proton, alpha, and neutron evaporation leads to a dispersion of reaction channels, particularly for high-angular-momentum input. Nevertheless, the study of high-spin states in light nuclei could be a rich and rewarding field.

We present here some preliminary results from our studies in the $A \sim 60$ region in which we have observed a collective rotational band in ^{65}Zn extending to spin $(41/2\hbar)$. This nucleus lies in a region of periodic table, where the shape is changing rapidly as a function of neutron and proton number. The proximity of the $N=38$ prolate and the $N=Z=34$, 36 oblate shell gaps implies that nuclei may exhibit different shapes at different excitation energies.

A spectacular study by Skoda *et al.* [24] on the $N=35$ ^{69}Se establishes a $g_{9/2}$ rotational band in this nucleus. By coupling a neutron to the triaxial ^{68}Se core ($\beta_2=0.3$), the nucleus ^{69}Se is driven to an experimentally proven oblate deformation, where the measured bandhead spin $9/2^+$ is argued to be formed by the valence neutron occupying the Nilsson orbital $9/2[404]$. Recently a study on the neighboring even-even isotope ^{64}Zn [1], finds a high-spin rotational band, which is observed to have two degenerate signature partners connected by strong $M1$ transitions. Nilsson-Strutinsky cranking calculations suggest a triaxial shape for this nucleus at intermediate spins. With increasing spin, the collectivity is gradually lost and two signatures end up in noncollective terminating states at $I=(25-26)\hbar$. One can thus expect that in odd- A ^{65}Zn , the odd neutron could couple to the triaxial core ^{64}Zn via polarization, similar to what happens for ^{69}Se ; thereby an oblate shape may evolve in the yrast configuration of ^{65}Zn . Moreover, in all the nuclei in this region [2-7], the positive-parity structure based on the $g_{9/2}$ orbital forms the

yrast line at high spins and, given the well-known understanding about the competition between shapes for this parity, it is of interest to follow the evolution of this structure to higher rotational frequencies.

The low-spin structure of the odd- A nucleus ^{65}Zn has been studied previously using both alpha-induced reactions [8,9] and various transfer reactions [10-12]. No heavy-ion-induced reaction has been attempted to explore the high-spin states for this nucleus. The most recent attempt to describe the structure of its low-lying levels [9] concluded that the first positive-parity level, the $J^\pi=9/2^+\hbar$ state at 1.065 MeV, can be interpreted as more than 90% of a $g_{9/2}$ quasineutron coupled to a zero-phonon excitation. Moreover, with an alpha projectile they could only populate up to the state at 5.769 MeV with no spin-parity assignment. The lifetime measurements of the $17/2_1^+\hbar$, $17/2_2^+\hbar$, and $21/2^+\hbar$ states at 3226, 3784, and 4934 keV energies, respectively, indicated an enhancement in the $B(E2)$ values of the 1173, 1731, and 1708 keV transitions and, hence, suggested the possibility of the onset of deformation at high spins. In order to investigate the possible shape changes in this nucleus, we have studied it to higher spin, which has established the predicted existence of collective bands for the first time.

II. EXPERIMENTAL PROCEDURE

The nucleus ^{65}Zn was studied at the Nuclear Science Centre-15UD pelletron facility using the $^{52}\text{Cr}(^{16}\text{O}, 2pn)^{65}\text{Zn}$ reaction at a beam energy of 65 MeV. The beam impinged on a natural (85% abundance) target of thickness 1 mg/cm^2 backed by a 7 mg/cm^2 thick gold foil. Prompt γ rays were collected using the Gamma Detector Array (GDA) [13] of 12 25%-efficient, high-purity Compton-suppressed germanium detectors (four at 45° , four at 99° , and four at 153°) located at the target position, in coincidence with the evaporated charged particles detected with the 4π Charged Particle Detector Array (CPDA) [14]. The CPDA, consisting of 14 phoswich ΔE - E detectors, selected the evaporation channels of the charged particles. The distance between the target and the HPGe detectors was about 18 cm. The resolution of these detectors was about 2 keV at 1332 keV. Initial calibrations were made with ^{60}Co ,

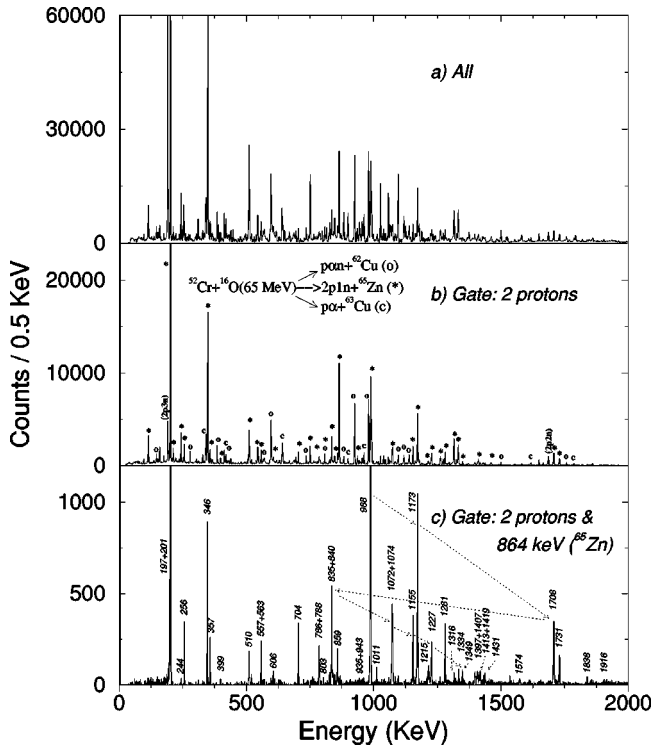


FIG. 1. γ -ray spectra (a) with no condition, (b) gated by two protons, and (c) gated by two protons and 864 keV transition of ^{65}Zn . Members of the $g_{9/2}$ yrast band (band 1) are indicated by the arrow in panel (c).

^{133}Ba , and ^{152}Eu sources, and during the experiment, on-line monitoring of the calibration was made using the known x rays and γ rays of gold, some strong γ lines of ^{62}Cu , ^{65}Zn , and 511 keV (e^+e^-). The $2pn$ evaporation channel leading to ^{65}Zn represented $\sim 22\%$ of the total fusion cross section.

III. DATA ANALYSIS AND RESULTS

Events were recorded when a trigger on twofold (or higher) clean γ coincidences in the Compton-suppressed array was issued. A total of 9.4×10^7 γ - γ -charged particle coincidence events were collected for an off-line analysis, from which γ - γ matrices were created by applying different gating conditions set on the number of detected protons and/or α particles [15,16]. The γ - γ coincidence relationship for ^{65}Zn was derived from a $4k \times 4k$ matrix gated on $2p$ reaction channel. A comparison of a typical projected γ spectrum from the total matrix (where no charged particle condition is used) with that of a $2p$ -gated matrix is shown in Fig. 1. Panels (a) and (b) in Fig. 1 present an ungated and $2p$ -gated γ -ray spectrum, respectively, while panel (c) shows the spectrum obtained by putting a gate on 864 keV transition of ^{65}Zn from the $2p$ -gated matrix. The only contaminants that could be identified in panel (b) of Fig. 1 are ^{62}Cu (αpn) [16] and ^{63}Cu (αp) [15], which were most abundantly produced in this reaction. The origin of this contaminants is clear. The leak through of these channels into the $2p$ -gated data arose from the occasional misidentification of a low-energy α particle as a proton in the charged particle detectors located at

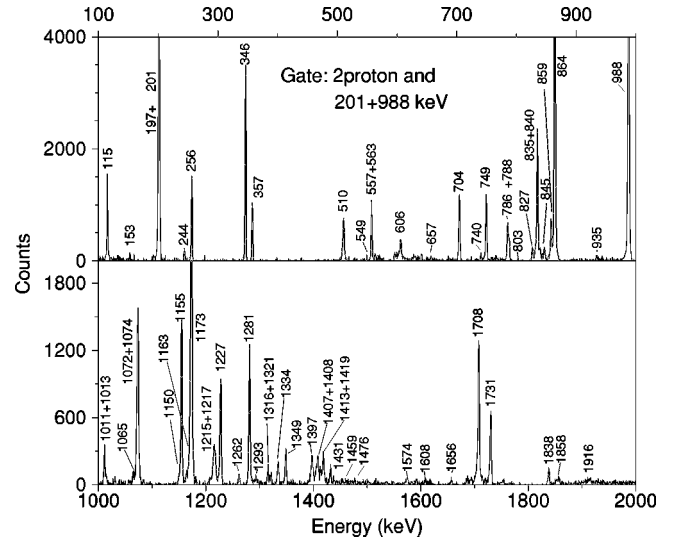


FIG. 2. Gamma-gamma coincidence spectrum for ^{65}Zn gated on a two-proton channel, highlighting the representative transitions of this nucleus.

backward angles relative to the beam axis.

A representative γ -ray spectrum of ^{65}Zn , deduced from a two-proton-gated matrix, is shown in Fig. 2, which is obtained by putting separate gates on 201 and 988 keV transitions of the most intense yrast cascade and summing them together. Coincidence, intensity balance, and summed energy relations were inspected to deduce the high-spin excitation scheme. The γ -ray energies and intensities presented in the level scheme (cf. Fig. 3) are based on the previously mentioned two-proton-gated γ - γ matrix. But for weak transitions and/or doublet structures, γ -gated spectra obtained from the total γ - γ matrix were considered. The spectrum analysis was performed using the code NSCSORT [17] developed at Nuclear Science Centre.

Spin and parity assignments were made on the basis of a DCO-type analysis [18] and from the known $5/2^- \hbar$ spin-parity value of the ground state. A separate γ - γ coincidence matrix was constructed with events detected in detectors at 153° (θ_1) versus those at 99° (θ_2) detectors. By gating a transition of known multipolarity on each axis of this matrix, a DCO ratio,

$$R_{DCO} = \frac{I_{\gamma_1}(\theta_1) \text{ gated by } \gamma_2(\theta_2)}{I_{\gamma_1}(\theta_2) \text{ gated by } \gamma_2(\theta_1)},$$

could be obtained. With this definition of R_{DCO} , for a quadrupole transition, when the gating transition is a known quadrupole, the ratio is expected to be approximately 1.0. A stretched dipole is expected to have R_{DCO} between 0.4 and 0.6, while a value between 0.6 and 0.8 implies a mixed transition. These limits are obtained by fitting the values for transitions of known multipolarity. Pure nonstretched dipole ($L=1, \Delta J=0$) transitions are also expected to have R_{DCO} values close to unity.

The decay scheme of ^{65}Zn derived from this work is shown in Fig. 3. Tentative spin and/or parity assignments are

TABLE I. Level energies (E_x), spin parity of the level (J^π), transition energies (E_γ), relative intensities of γ -ray transitions (I_γ), and DCO ratios (R_{DCO}) are shown for ^{65}Zn . Level energies are given to the nearest keV. The error in the transition energy is about 0.1 keV. New γ transitions and energy levels are marked by asterisks (*).

E_x (keV)	J^π (\hbar)	E_γ (keV)	I_γ (%)	R_{DCO}	E_x (keV)	J^π (\hbar)	E_γ (keV)	I_γ (%)	R_{DCO}
54	$1/2^-$				5340*	$21/2^+$	1261.8*	1.6 ± 0.3	1.3 ± 0.5
115	$3/2^-$	114.9	5.1 ± 0.6	0.5 ± 0.3	5411	$23/2^+$	346.0	11.6 ± 0.4	0.6 ± 0.1
207	$3/2^-$	153.0	3.0 ± 1.0				787.8*	3.1 ± 0.4	0.4 ± 0.4
864	$7/2^-$	657.3	3.4 ± 0.5		5668*	$25/2^+$	256.0*	4.7 ± 0.7	0.5 ± 0.4
		749.0	9.6 ± 0.4	1.4 ± 0.2	5769	$25/2^+$	357.2*	3.8 ± 0.8	0.6 ± 0.4
		864.1	88.1 ± 0.2	0.6 ± 0.1			704.2*	7.7 ± 0.5	0.9 ± 0.3
1047	$5/2^-$	932.1	1.1 ± 0.6				835.0	18.1 ± 0.4	0.9 ± 0.1
1065	$9/2^+$	201.3	100 ± 0.3	0.5 ± 0.1	5805*		740.1*	1.2 ± 0.5	
		1065.1	5.3 ± 0.7		6280*	$25/2^+$	510.2*	4.6 ± 0.4	0.3 ± 0.2
1263	$9/2^-$	197.0	1.6 ± 0.8				1215.1*	3.4 ± 1.2	0.9 ± 0.3
		399.2	1.0 ± 0.6				1656.2*	2.9 ± 0.4	
2053	$13/2^+$	987.8	78.1 ± 0.1	1.0 ± 0.1	6524*	$(25/2^+)$	244.0*	1.1 ± 0.3	
2137	$11/2^+$	1072.1	9.0 ± 1.4	0.4 ± 0.3			1459.0*	1.2 ± 0.6	
2923	$13/2^+$	785.7	5.4 ± 0.8	0.7 ± 0.3	6753*	$(25/2^+)$	1412.8*	1.4 ± 0.5	1.2 ± 0.5
		1857.8	7.0 ± 1.0	1.2 ± 0.3	6843*	$29/2^+$	563.0*	2.1 ± 0.5	
3226	$17/2^+$	1172.7	45.0 ± 0.2	1.0 ± 0.1			1073.6*	12.0 ± 1.9	1.1 ± 0.1
3472	$15/2^+$	548.9*	1.3 ± 0.5				1173.0	3.0 ± 0.5	
		1334.0	3.8 ± 0.9				1431.3*	2.4 ± 0.4	
		1418.6	3.3 ± 0.7		6985*	$29/2^+$	1216.7*	3.5 ± 0.5	0.9 ± 0.4
3784	$17/2^+$	557.3	5.7 ± 0.9				1315.6*	1.8 ± 0.9	
		858.7*	5.1 ± 0.8	1.4 ± 0.4	7062*	$(29/2^+)$	1293.2*	1.5 ± 0.7	1.6 ± 0.5
		1730.6	9.3 ± 1.1	1.1 ± 0.3	7687*	$29/2^+$	845.2*	1.6 ± 0.5	
4078	$17/2^+$	605.9	2.6 ± 0.8				1163.4*	1.2 ± 0.5	
		1154.7	5.0 ± 0.4	1.0 ± 0.5			1407.3*	3.6 ± 0.9	1.3 ± 0.4
4238 *	$(21/2^+)$	1011.0*	3.0 ± 1.0	1.1 ± 0.5			1916.1*	2.0 ± 0.8	
4547 *		1320.6*	1.8 ± 0.2		7998*	$33/2^+$	934.8*	0.5 ± 0.4	
4625 *	$21/2^+$	849.7*	1.1 ± 0.5				1012.7*	1.0 ± 0.3	
		1397.0*	4.5 ± 0.5	1.3 ± 0.3			1154.7*	11.1 ± 1.2	1.2 ± 0.2
4703 *		1476.3*	1.4 ± 0.7		8327*	$(29/2^+)$	1573.7*	1.4 ± 0.8	0.9 ± 0.6
4880 *	$(19/2^+)$	803.0*	1.2 ± 0.4		8594*		1607.8*	1.0 ± 0.3	
		1407.8*	1.5 ± 0.3	1.2 ± 0.6	9225*	$37/2^+$	1227.0*	10.5 ± 0.8	1.2 ± 0.1
4934	$21/2^+$	1150.3*	1.7 ± 0.5		10574*	$(41/2^+)$	1348.6*	3.8 ± 0.3	0.9 ± 0.4
		1707.8	18.9 ± 1.0	0.9 ± 0.1					
5065	$21/2^+$	439.9*	1.0 ± 0.5						
		826.8*	2.6 ± 0.6						
		1280.8	13.5 ± 1.1	1.2 ± 0.1					
		1837.9*	3.8 ± 0.6	1.0 ± 0.5					

occur at high angular momenta. Many of these effects have a straightforward interpretation in terms of the interplay between deformation, pairing, and the Coriolis force. Moreover, both protons and neutrons lie in the same $g_{9/2}$ high- j subshell in this region. Consequently, proton and neutron band crossings are expected at similar frequencies. For γ soft systems such configuration changes induce strong shape variations caused by aligned quasiparticles which polarize the core. The valence quasiparticle orbitals belonging to

high- j unique parity subshells exert strong γ -driving forces on the core.

In odd- A nuclei in this mass region, very strong polarization effects coming from aligned quasiparticles excitations have been observed [6,7,19–23]. A spectacular example of quasiparticle alignment related to γ softness has recently been established in ^{69}As [7]. According to the calculations, the excitation energy of the odd $g_{9/2}$ proton in ^{69}As favors near-oblate shape ($\gamma \sim -55^\circ$) for the ($\alpha = 1/2$) band. Shape

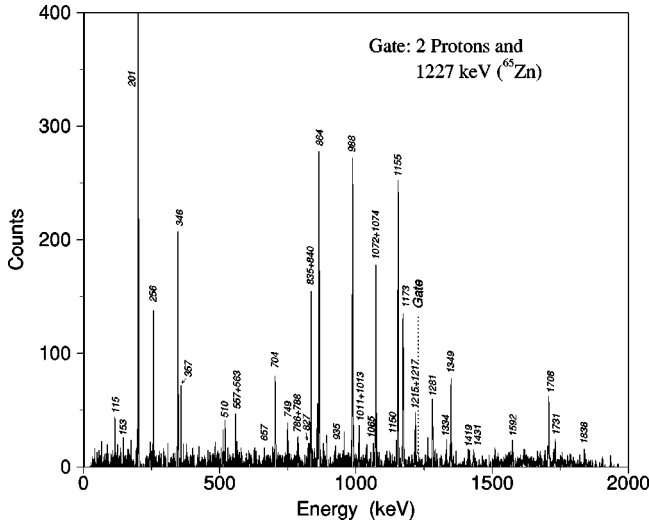


FIG. 4. Spectrum of γ rays in coincidence with two protons and 1227 keV transition, a higher-lying member of $g_{9/2}$ band in ^{65}Zn .

properties of the even-even isotope ^{64}Zn have recently been discussed in Ref. [1], where it has been shown that the nucleus is well deformed ($\beta_2=0.3$) in its ground state, evolving to a noncollective triaxial shape after the first band crossing. One can thus expect that in ^{65}Zn different quasi-particle excitations would polarize the nuclear shape towards different regions in the (β_2, γ) plane. A similar kind of situation was observed recently in the $N=35$ isotope, ^{69}Se [24], where the large oblate deformation ($\beta_2 \sim -0.3$) measured in the $g_{9/2}$ band is interpreted to be generated by the odd neutron coupled to the triaxial ^{68}Se core [25] via polarization.

A. Cranked shell model analysis

Alignments and structural changes due to rotation are more clearly seen by using the cranked shell model (CSM). Kinematical moment of inertia, $J^{(1)} = i_x / \omega$, and alignment, $i = i_x - i_{ref}$, for the positive parity bands of ^{65}Zn are shown in Fig. 5. Also shown are alignments, for comparison, for the yrast bands in the neighboring nuclei ^{67}As [6], ^{68}Ge [26], and ^{69}As [7]—all of which were reported to have near-oblate ground-state deformations. Two K values are used for the data for ^{65}Zn since for triaxial deformation, the K value is not well defined. A K value of 0.5 corresponds to prolate deformation while the high- K value corresponds to oblate deformation. It is only now with the extension of the band structure in ^{65}Zn that an alignment can be fully established. Indeed, it is evident from Fig. 5 that there is a gain in alignment of $\sim 7\hbar$ at a frequency of 0.60 MeV. The beginning of analogous backbends are also observed in $^{67,69}\text{As}$. This suggests a similarity in structure, perhaps related to similarity in shape. In ^{68}Ge the levels up to $J^\pi = 6^+\hbar$ have been compared with EXVAM calculations and interpreted as almost pure oblate states [27]. However, above $8^+\hbar$, one neutron-aligned band is consistent with the prediction that the contribution of the $g_{9/2}$ neutrons and protons to the total angular momentum should be nearly equal. This configuration is calculated to have a prolate shape after crossing [28].

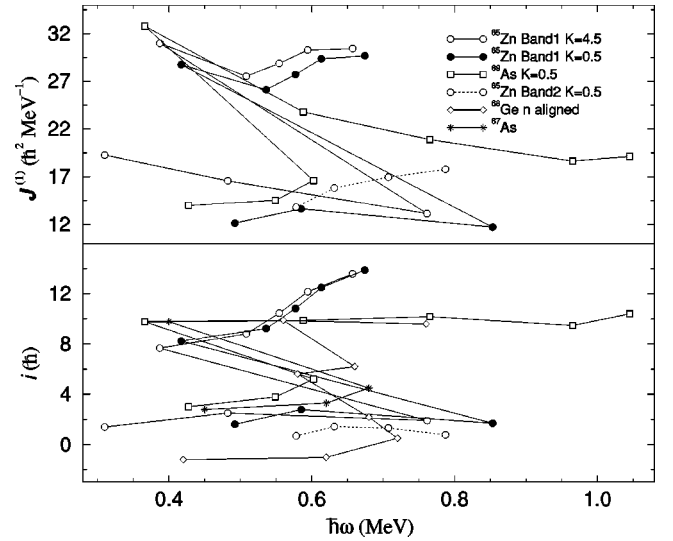


FIG. 5. Experimentally deduced kinematic moments of inertia ($J^{(1)}$) and alignments (i) for the rotational bands in ^{65}Zn , $^{67,69}\text{As}$ [19,20], and ^{68}Ge [28]. Harris reference parameters of $J_0 = 6.0\hbar^2 \text{ MeV}^{-1}$ and $J_1 = 3.5\hbar^4 \text{ MeV}^{-3}$ have been used for all nuclei.

The level scheme for ^{65}Zn , as shown in Fig. 3, shows that the nucleus has a $J^\pi = 5/2^- \hbar$ ground state. This is interpreted as a neutron in the $5/2^- [303]$ Nilsson orbital, and in order for this orbit to approach the Fermi surface, an oblate shape is required. The $J^\pi = 9/2^+ \hbar$ state at 1.065 MeV is the band-head for the $g_{9/2}$ band and the level scheme already shows that there is a change in alignment as the excitation energy increases in this band. The gain in alignment, as shown in Fig. 5, is $\sim 7\hbar$, which is consistent with the alignment of a pair of $g_{9/2}$ particles. However, since ^{65}Zn has an odd number of neutrons, the first neutron $g_{9/2}$ crossing is blocked and the alignment observed must be that of a pair of $g_{9/2}$ protons. The maximum value of alignment which can be obtained from a pair of $g_{9/2}$ particles is $8\hbar$ and the fact that almost all of this alignment is observed suggests that the aligning particles must occupy low- Ω orbitals. This indicates that the nucleus is prolate with the low- $\Omega g_{9/2}$ $1/2[440]$ orbital near the Fermi surface. In the present case, when the nuclear shape is rather soft, the proton alignment will polarize the nuclear shape towards more noncollective shapes.

B. Woods-Saxon calculations

A theoretical analysis of the $g_{9/2}$ rotational band in ^{65}Zn has been performed using the Woods-Saxon cranking model of Ref. [29]. Equilibrium shapes were calculated by minimizing the total Routhian with respect to deformation parameters β_2 , β_4 , and γ . As a residual interaction, the monopole pairing force has been taken with the strength from Ref. [29]. At zero frequency self-consistent pairing gaps were calculated within the BCS model. At higher rotational frequencies, however, the pairing gaps were allowed to decrease gradually with increasing rotational frequency according to a simple analytical formula [29]. The Fermi surfaces for protons and neutrons have been found numerically at each fre-

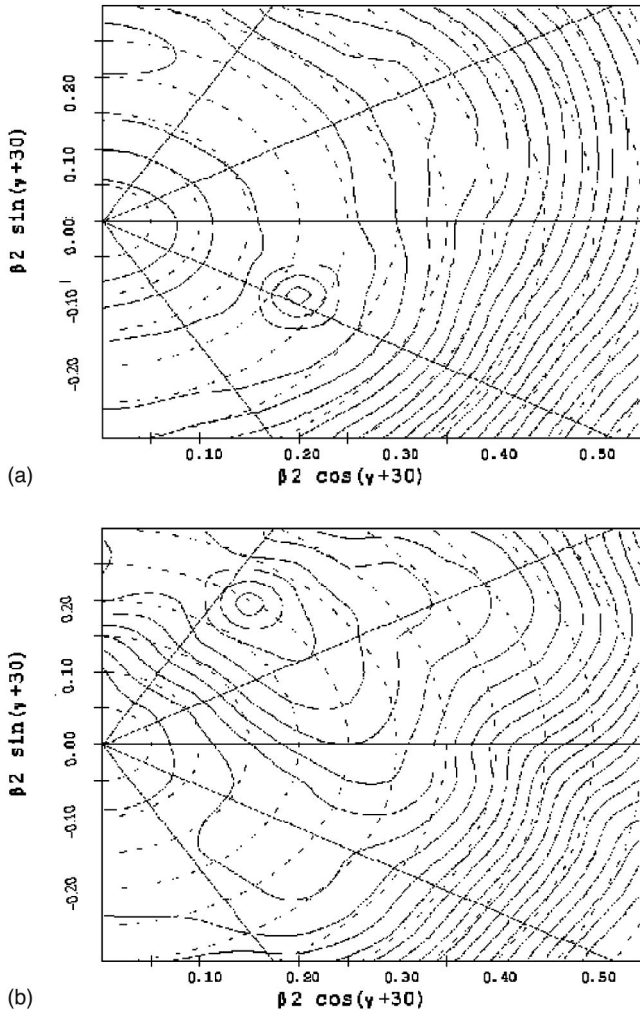


FIG. 6. Total Routhian Surface calculations for the positive-parity, $\alpha = +1/2$ structure in ^{65}Zn at a rotational frequency of 0.20 MeV (a) and 0.65 MeV (b). The contours trace shapes of the equipotential and are separated by 0.20 MeV.

quency from the particle number equation. The total Routhian in a fixed quasiparticle configuration (defined by means of parity, signature, and excitation quantum numbers) was defined as a sum of Strunsky energy (liquid drop plus shell correction) and the rotational energy. The Hartree-Fock-Bogoliubov code of Nazarewicz *et al.* [29] is used for the calculations. The Total Routhian Surface (TRS) is calculated at each $\hbar\omega$ in the β_2 - γ plane with minimization on β_4 . Figure 6 shows TRS calculations for the positive parity, $\alpha = +1/2$ sequence in ^{65}Zn . The predicted shape at low frequency ($\hbar\omega = 0.20$ MeV) is oblate ($\gamma \sim -55^\circ$), with a β_2 of ~ 0.22 [Fig. 6(a)] but as the rotational frequency increases the nucleus first becomes γ soft and then ($\hbar\omega = 0.65$ MeV) triaxial prolate ($\gamma \sim 22^\circ$) with a β_2 deformation of about ~ 0.25 [Fig. 6 (b)]. At higher spins ($\sim 17\hbar$), a new structure emerges in the calculations, corresponding to a β_2 value of ~ 0.37 ; there, an additional pair of particles is supposed to move from the $f_{7/2}$ into the $g_{9/2}$ orbits, inducing almost superdeformed states. In our experiment, however, we could not populate the superdeformed states predicted by the TRS calculations.

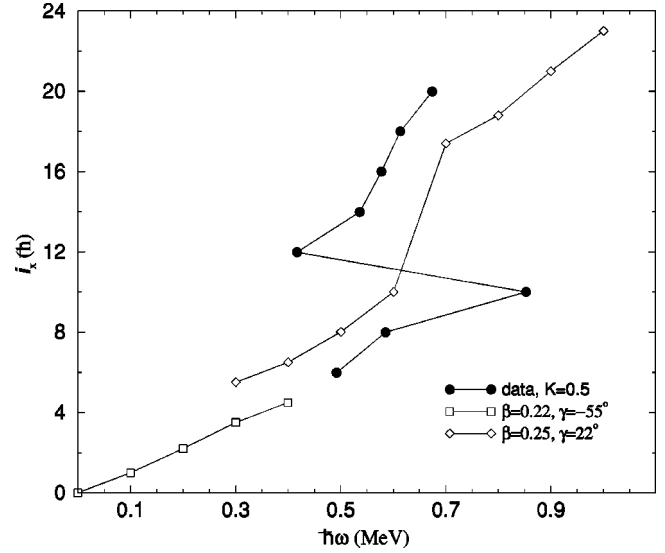


FIG. 7. A comparison between experimental values of i_x and those calculated for the configurations in the minima shown in Fig. 6. The solid points show the experimental values for the $g_{9/2}$ band in ^{65}Zn .

Figure 7 shows a plot of the calculated projection of the total angular momentum on the x axis (i_x), for the configurations in the minima shown in Fig. 6, as a function of rotational frequency. Also shown are the experimental values where $i_x = \sqrt{I(I+1) - K^2}$. It is interesting to note that at low values of frequency the experimental values are quite close to the data points for the oblate shapes (open squares) and that after the backbend they follow nicely the trend of the calculation corresponding to triaxial shapes (open diamond). On the basis of these data and the calculations shown in Fig. 6, it can be concluded that there is evidence for a shape change in this nucleus from oblate shapes at low spin to triaxial-prolate shapes at intermediate spin. At higher angular momenta, we observe an increase of i_x in experiment, which is not reproduced in the calculations.

To investigate the nature of the yrast band and to predict correctly the crossing frequency, we have calculated the crossing frequencies for different shape parameters for protons and neutrons in ^{65}Zn , which have been plotted in Fig. 8. The inset shows the variation of proton and neutron crossing frequencies as a function of β_2 for both prolate ($\gamma = 0^\circ$) and oblate ($\gamma = -55^\circ$) shapes. It is evident that proton crossing has a minimum value of 0.60 MeV for a near-oblate deformation of $\beta_2 \sim 0.22$, and this increases for both lower and higher values of β_2 . While in Fig. 8 the proton crossing is seen to decrease with increasing triaxiality in the direction of a negative γ value. Thus a quasineutron configuration seems to be more likely for the yrast band of ^{65}Zn , which becomes three quasiparticle in nature after the alignment of two protons at $\hbar\omega \sim 0.60$ MeV.

The nucleus ^{65}Zn has two protons and seven neutrons outside the doubly magic core ^{56}Ni . In the valence configurations, the active orbitals are those of the $N=3$ $p_{3/2}$, $f_{5/2}$, and $p_{1/2}$ subshells and the $N=4$ $g_{9/2}$ intruder subshell. High-spin states can be understood in terms of a $\nu[g_{9/2}^3 - (f_{5/2}$

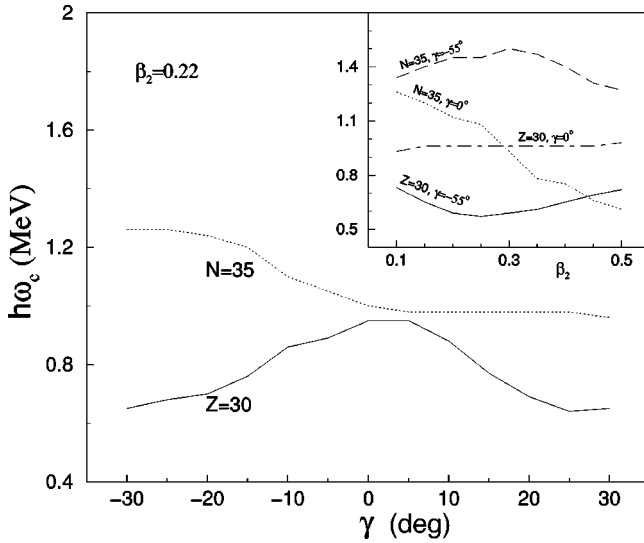


FIG. 8. Calculated crossing frequencies ($\hbar\omega$) for protons and neutrons in ^{65}Zn as a function of triaxiality parameter (γ) and (inset) axial deformation (β_2).

$-p_{3/2}^4 \otimes \pi[g_{9/2}^2]$ particle structure with respect to ^{56}Ni . This structure terminates at $I^\pi = 49/2^+$ state. This state is not observed in our data set. However, the state below ($I^\pi = 41/1^+$), having the proton-neutron $(p_{3/2})^2 - 2^+$ not fully aligned, is close in energy to the corresponding collective state. It is therefore most likely that we observe a transition into the noncollective sector (perhaps brought about by mixing with the noncollective states) at oblate shapes just below the terminating $I^\pi = 49/2^+$ state.

V. CONCLUSIONS

The high-spin states of ^{65}Zn have been studied with the GDA + CPDA configuration, identifying previously unobserved states up to an excitation energy of 10.574 MeV. The present investigation has resulted in the placement of 42 new γ rays and 20 new levels in the decay scheme of ^{65}Zn . Moreover, we have observed a $g_{9/2}$ rotational band and established an alignment of $\sim 7\hbar$ at a frequency of 0.60 MeV. This is interpreted as the alignment of a pair of $g_{9/2}$ protons. Consideration of the spin projection for this configuration provides evidence of shape changes in this nucleus from an oblate shape to a triaxial prolate shape at intermediate spin where the nucleus is stabilized by quasiparticle alignment. This is confirmed by the calculations using the Woods-Saxon-Bogoliubov cranking model. The results show that at low spins the yrast structure of ^{65}Zn is consistent with a near-oblate shape with a deformation $\gamma \sim -55^\circ$. The alignment of a $g_{9/2}$ proton pair triggers a shape change towards less collective triaxial configurations with $\gamma \sim 22^\circ$. This phenomenon is similar to those in ^{67}As [6], ^{68}Ge [26], and ^{69}As [7] in this mass region, where neutron alignment causes a shape change from near-oblate to near-prolate shapes. In ^{65}Zn , however, it is the $g_{9/2}$ proton alignment that triggers the shape change.

ACKNOWLEDGMENTS

The authors wish to thank the operating crew of the Pelletron facility at the Nuclear Science Centre. Special thanks are due to Prof. N. Singh (P.U.), Dr. S.K. Datta, Dr. G. Mukherjee, D. Kabiraj, and P. Barua for different kinds of help during and after the experiment. One of the authors (B.M.) gratefully acknowledges a research grant from the University Grants Commission (India).

- [1] A. Galindo-Uribarri, D. Ward, G. C. Ball, V. P. Janzen, D. C. Radford, I. Ragnarsson, and D. Headly, *Phys. Lett. B* **422**, 45 (1998).
- [2] C. E. Svensson *et al.*, *Phys. Rev. Lett.* **79**, 1233 (1997).
- [3] C. E. Svensson *et al.*, *Phys. Rev. Lett.* **80**, 2558 (1998).
- [4] C. E. Svensson *et al.*, *Phys. Rev. Lett.* **82**, 3400 (1999).
- [5] M. Devlin *et al.*, *Phys. Rev. Lett.* **82**, 5217 (1999).
- [6] T. F. Lang, D. M. Moltz, J. E. Reiff, J. C. Batchelder, J. Carney, J. D. Robertson, and C. W. Beausang, *Phys. Rev. C* **42**, R1175 (1990).
- [7] A. M. Bruce *et al.*, *Phys. Rev. C* **62**, 027303 (2000).
- [8] A. Nilsson and Z. P. Sawa, *Phys. Scr.* **9**, 83 (1974).
- [9] P. Banerjee, B. Sethi, M. B. Chatterjee, and R. Goswami, *Phys. Rev. C* **50**, 1813 (1994).
- [10] A. Kogan, P. R. G. Lornie, G. D. Jones, M. R. Nixon, H. G. Price, R. Wadsworth, and P. J. Twin, *J. Phys. G* **4**, 755 (1978).
- [11] A. Charvet, J. Sau, R. Duffait, and R. Chery, *Phys. Rev. C* **15**, 1679 (1977).
- [12] G. F. Neal, Z. P. Sawa, and P. R. Chagnon, *Nucl. Phys. A* **295**, 351 (1978).
- [13] S. C. Pancholi and R. K. Bhowmik, *Indian J. Pure Appl. Phys.* **27**, 660 (1989).
- [14] S. Muralithar *et al.*, in *Proceedings of the DAE Symposium on Nuclear Physics, India, 1998*, Vol. 41B, p. 404.
- [15] B. Mukherjee, S. Muralithar, R. P. Singh, R. Kumar, K. Rani, S. C. Pancholi, and R. K. Bhowmik, *Pramana, J. Phys.* **55**, L471 (2000).
- [16] B. Mukherjee, S. Muralithar, R. P. Singh, R. Kumar, K. Rani, and R. K. Bhowmik, *Phys. Rev. C* **63**, 057302 (2001).
- [17] R. K. Bhowmik (private communication).
- [18] A. Kramer-Flecken, T. Morek, R. M. Lieder, W. Gart, G. Hebbinghaus, H. M. Jager, and W. Urban, *Nucl. Instrum. Methods Phys. Res. A* **275**, 333 (1989).
- [19] R. S. Zigelboim, S. G. Buccino, F. E. Durham, J. Doring, P. D. Cottle, J. W. Holcomb, T. D. Johnson, S. L. Tabor, and P. C. Womble, *Phys. Rev. C* **50**, 716 (1994).
- [20] M. Wiosna, J. Busch, J. Eberth, M. Liebchen, T. Mylaeus, N. Schmal, R. Sefzig, S. Skoda, and W. Teichert, *Phys. Lett. B* **200**, 255 (1988).
- [21] M. S. Kaplan, J. X. Saladin, D. F. Winchell, H. Takai, and J. Dudek, *Phys. Rev. C* **44**, 668 (1991).
- [22] T. D. Johnson, T. Glasmacher, J. W. Holcomb, P. C. Womble, and S. L. Tabor, *Phys. Rev. C* **42**, 516 (1992).
- [23] G. N. Sylvan, J. E. Purcell, J. Doring, J. W. Holcomb, G. D.

- Johns, T. D. Johnson, M. A. Riley, P. C. Womble, V. A. Wood, and S. L. Tabor, *Phys. Rev. C* **48**, 2252 (1993).
- [24] S. Skoda *et al.*, *Nuovo Cimento A* **111**, 669 (1998).
- [25] S. M. Fischer, D. P. Balamuth, P. A. Hausladen, C. J. Lister, M. P. Carpenter, D. Seweryniak, and J. Schwartz, *Phys. Rev. Lett.* **84**, 4046 (2000).
- [26] D. Ward *et al.*, *Phys. Rev. C* **63**, 014301 (2000).
- [27] A. Petrovici, K. W. Schmid, F. Grummer, and A. Faessler, *Nucl. Phys.* **A517**, 108 (1990).
- [28] U. Hermkens, F. Becker, J. Eberth, S. Freund, T. Mylaes, S. Skoda, W. Tiechert, and A.v.d. Werth, *Z. Phys. A* **343**, 71 (1992).
- [29] W. Nazarewicz, J. Dudek, R. Bengtsson, T. Bengtsson, and I. Ragnarsson, *Nucl. Phys.* **A435**, 397 (1985).